



Full paper / Mémoire

Mechanism of the palladium-catalysed electrosynthesis of diethyl carbonate from carbon monoxide and ethanol

Christian Amatore ^{a,*}, Samia Bensalem ^a, Said Ghalem ^b, Anny Jutand ^{a,*},
Daniele Fenech ^c, Alessandro Galia ^c, Giuseppe Silvestri ^c

^a Département de chimie, UMR CNRS 8640, École normale supérieure, 24, rue Lhomond, 75231 Paris cedex 05, France

^b Département de chimie, faculté des sciences, université de Tlemcen, BP 119, 13000 Tlemcen, Algérie

^c Dipartimento di Ingegneria Chimica dei Processi e dei Materiali, Università di Palermo, Via delle Scienze, 90128 Palermo, Italy

Received 20 March 2003; accepted 1 August 2003

Available online 13 August 2004

Abstract

A mechanism is proposed for the PdBr₂(PPh₃)₂-catalysed electrosynthesis of diethyl carbonate from carbon monoxide and ethanol, proceeding at room temperature and atmospheric CO pressure. The mechanism is investigated by cyclic voltammetry and ³¹P NMR spectroscopy. The active Pd⁰ complex able to coordinate CO is generated by the chemical reduction of PdBr₂(PPh₃)₂ by EtO⁻ ions generated from EtOH at the cathode. After reaction of EtO⁻ ions with Pd⁰(PPh₃)₂(CO), the ensuing anionic complex [(PPh₃)₂Pd⁰-COOEt]⁻ is oxidized at the anode in a key step leading to BrPd^{II}-COOEt(PPh₃)₂. A nucleophilic attack of ethoxide on the latter generates diethyl carbonate and the Pd⁰ complex active in the catalytic cycle. **To cite this article:** C. Amatore et al., C. R. Chimie 7 (2004).

© 2004 Académie des sciences. Published by Elsevier SAS. All rights reserved.

Résumé

Un mécanisme est proposé pour l'électrosynthèse du carbonate de diéthyle à partir de monoxyde de carbone et d'éthanol, catalysée par PdBr₂(PPh₃)₂ et procédant à température ambiante et pression atmosphérique de CO. Le mécanisme est étudié par voltamétrie cyclique et par spectroscopie RMN ³¹P. Le complexe du Pd⁰ capable de coordonner CO est généré par la réduction chimique de PdBr₂(PPh₃)₂ par les ions EtO⁻ formés à la cathode, à partir de l'éthanol. Après réaction des ions EtO⁻ avec Pd⁰(PPh₃)₂(CO), le complexe anionique formé [(PPh₃)₂Pd⁰-COOEt]⁻ est oxydé à l'anode conduisant au complexe BrPd^{II}-COOEt(PPh₃)₂. Une attaque nucléophile des ions éthylate sur ce dernier donne du carbonate de diéthyle et le complexe du Pd⁰ impliqué dans le cycle catalytique. **Pour citer cet article :** C. Amatore et al., C. R. Chimie 7 (2004).

© 2004 Académie des sciences. Published by Elsevier SAS. All rights reserved.

Keywords: Palladium; Carbon monoxide; Carbonylation; Electrosynthesis; Voltammetry

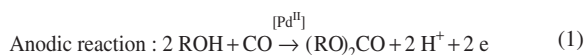
Mots clés : Palladium ; Monoxyde de carbone ; Carbonylation ; Électrosynthèse ; Voltamétrie

* Corresponding author.

E-mail addresses: christian.amatore@ens.fr (C. Amatore), anny.jutand@ens.fr (A. Jutand).

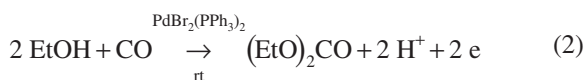
1. Introduction

Transition-metal salts or complexes catalyse the electrosynthesis of dialkyl carbonate from alcohols and carbon monoxide [1] including Palladium salts or complexes [2,3] (Eq. (1)). This anodic process proceeds in methanol or ethanol under mild conditions i.e., at room temperature and with CO at atmospheric pressure, leading to dimethyl carbonate (DMC) [2] and diethyl carbonate (DEC) respectively [3].



This process is an alternative to procedures involving chemical oxidants such as oxygen [4–6], which generally require more drastic conditions (high temperatures and high CO pressures) or electrolytic carbonylation in the gas phase [7,8]. The mechanism of alcohols carbonylation involving stoichiometric amounts of Pd^{II} complexes has been reported. It proceeds via the formation of intermediate alkoxy-carbonyl complexes XPd^{II}(COOR)L₂ (X = Cl, OAc; L = PPh₃, dppe; R = Me, Et) obtained from Pd^{II} complexes under high CO pressures and high temperatures. In the presence of a base (trialkylamine) and alcohol, they evolve to dialkyl carbonates and Pd⁰ complexes [9–12]. The process is not catalytic in the absence of any oxidants.

We report here a mechanism for the electrosynthesis of diethyl carbonate from ethanol and CO catalysed



by PdBr₂(PPh₃)₂, performed at room temperature and atmospheric pressure of CO (Eq. (2)) [2,3]. It has been investigated by cyclic voltammetry associated to ³¹P NMR spectroscopy.

The electrosynthesis was more efficient in the presence of catalytic amounts of PdBr₂ [2,3]. However, the reduction of PdBr₂ observed by cyclic voltammetry resulted in poor resolved voltammograms due to a lack of stabilization of the electrogenerated Pd⁰ that deposited at the electrode. Consequently the mechanism has been investigated with PdBr₂(PPh₃)₂ as catalyst.

2. Results and discussion

The electrosynthesis of diethyl carbonate proceeds at the anode. The concomitant cathodic process could

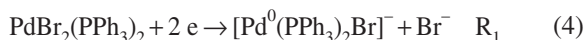
be either the reduction of PdBr₂(PPh₃)₂ or the reduction of protons generated from EtOH. A cyclic voltammetry of a solution of PdBr₂(PPh₃)₂ (2 mM) in ethanol (containing *n*Bu₄NBF₄, 0.3 M) did not exhibit any reduction peak before the reduction of ethanol starting at –1.4 V/SCE. Consequently, the cathodic process did not involve the reduction of PdBr₂(PPh₃)₂ to a Pd⁰ complex but the deprotonation of EtOH into EtO[–] (Eq. (3)) via the reduction of H⁺:



Cyclic voltammetry was selected as the analytical technique to monitor the fate of PdBr₂(PPh₃)₂ in the course of the electrosynthesis. Because the catalytic precursor PdBr₂(PPh₃)₂ could not be characterized in ethanol by cyclic voltammetry (vide supra), the mechanism of the electrosynthesis was investigated in THF to be able to monitor reactions of PdBr₂(PPh₃)₂ with any reagents involved in the catalytic process i.e., CO and/or EtO[–].

2.1. Investigation of the reaction of PdBr₂(PPh₃)₂ with CO in the absence and presence of PPh₃ (2 equiv)

The complex PdBr₂(PPh₃)₂ (2 mM) in THF (containing *n*Bu₄NBF₄, 0.3 M) was characterized by a single overall bielectronic reduction peak R₁ at E^p_{R1} = –0.875 V/SCE (gold disk electrode, i.d. 0.5 mm, scan rate: 0.2 V s^{–1}). An oxidation peak O₁ located at +0.100 V/SCE was observed on the reverse scan (Fig. 1a, full line). We have reported that the electrochemical reduction of PdBr₂(PPh₃)₂ generates an anionic complex [Pd⁰(PPh₃)₂Br][–] oxidized at O₁ (Eqs. (4) and (5)) [13].



In the presence of excess PPh₃ (2 equiv), the reduction peak R₁ was not significantly modified, whereas the oxidation peak current intensity of the electrogenerated Pd⁰ complex located at O₁ was slightly higher than in absence of PPh₃, due to a stabilization of the electrogenerated Pd⁰ complex by PPh₃ (Eq. (6)) [13].



Carbon monoxide was then bubbled into the cell to investigate any reaction of PdBr₂(PPh₃)₂ with CO –

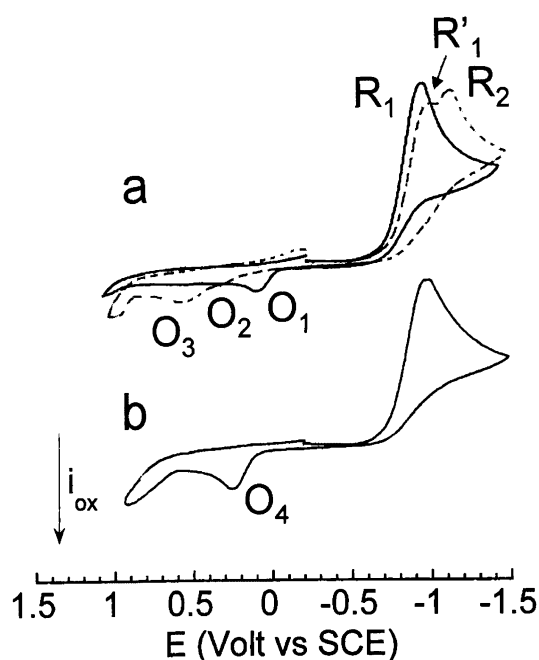
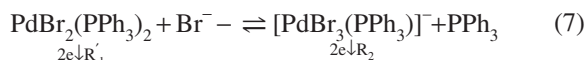


Fig. 1. Cyclic voltammetry performed in THF (containing $n\text{Bu}_4\text{NBF}_4$, 0.3 mol dm^{-3}) at a steady gold disk electrode (i.d. 0.5 mm) with a scan rate of 0.2 V s^{-1} at 25°C . Reduction first: (a) (—) $\text{PdBr}_2(\text{PPh}_3)_2$ (2 mmol dm^{-3}); (---) $\text{PdBr}_2(\text{PPh}_3)_2$ (2 mmol dm^{-3}) and CO (1 atm). b) $\text{PdBr}_2(\text{PPh}_3)_2$ (2 mmol dm^{-3}), PPh_3 (4 mmol dm^{-3}) and CO (1 atm).

complexation [12] or reduction. In the presence of CO , the reduction peak R_1 of $\text{PdBr}_2(\text{PPh}_3)_2$ was slightly shifted to more negative potential ($E_{R_1}^p = -0.895 \text{ V}$) with a lower peak current (Fig. 1a, dashed voltammogram). A new reduction peak R_2 of small intensity appeared at more negative potential, $E_{R_2}^p = -1.025 \text{ V}$ (Fig. 1a, dashed voltammogram). This suggests that, in the presence of CO , bromide ions were released in higher amount in the reduction of $\text{PdBr}_2(\text{PPh}_3)_2$ (Eq. (4)) than in the absence of CO . As reported, Br^- ions react with $\text{PdBr}_2(\text{PPh}_3)_2$ and expel one PPh_3 to generate an anionic Pd^{II} complex $[\text{Pd}^{\text{II}}\text{Br}_3(\text{PPh}_3)]^-$ (Eq. (7)) [14] less easily reduced at R_2 .

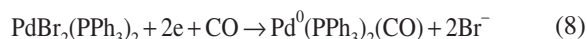


The potential shift observed from R_1 to R'_1 for $\text{PdBr}_2(\text{PPh}_3)_2$ is a consequence of its involvement in the equilibrium in Eq. (7) (CE mechanism).

The complex $\text{PdBr}_2(\text{PPh}_3)_2$ was thus rather stable in THF in the presence of bubbling CO , because the

overall reduction current of $\text{PdBr}_2(\text{PPh}_3)_2$ did not decrease with time (the current intensity of R'_1 being proportional to $\text{PdBr}_2(\text{PPh}_3)_2$ concentration). Consequently, at room temperature and atmospheric CO pressure, complexation of $\text{PdBr}_2(\text{PPh}_3)_2$ by CO did not occur. It is known that CO can reduce Pd^{II} salts to Pd^0 [15] but when ligated by phosphine, as in $\text{PdBr}_2(\text{PPh}_3)_2$, the reduction by CO (under atmospheric pressure) did not occur in the time scale investigated here (1 h). The reduction of $\text{PdCl}_2(\text{PPh}_3)_2$ by CO does not occur even at high CO pressure [12]. No oxidation peak was detected when the scan was performed to oxidation first.

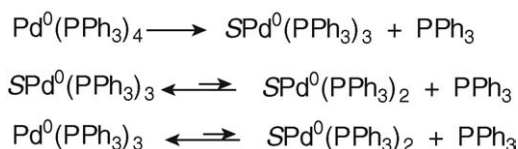
One notices that in the presence of CO , the oxidation peak O_1 of $[\text{Pd}^0(\text{PPh}_3)_2\text{Br}]^-$, generated by the reduction of $\text{PdBr}_2(\text{PPh}_3)_2$, disappeared and two new oxidation peaks O_2 ($E_{O_2}^p = +0.365 \text{ V}$) and O_3 ($E_{O_3}^p = +0.595 \text{ V}$) were detected (Fig. 1a, dashed voltammogram). The latter was assigned to the oxidation of bromide ions by comparison to an authentic sample of $n\text{Bu}_4\text{NBr}$. This confirms that, in the presence of CO , the electrochemical reduction of $\text{PdBr}_2(\text{PPh}_3)_2$ did not generate the anionic $[\text{Pd}^0(\text{PPh}_3)_2\text{Br}]^-$ complex but a new Pd^0 complex, assigned to $\text{Pd}^0(\text{PPh}_3)_2(\text{CO})$ (Eq. (8)), which was oxidized at O_2 . However, its small oxidation peak current indicates that $\text{Pd}^0(\text{PPh}_3)_2(\text{CO})$ was not very stable within the time scale of the cyclic voltammetry, due to the lack of stabilizing ligand or to insufficient CO pressure (Eq. (9), $S = \text{solvent}$).



The existence of the equilibrium in Eq. (9) has been evidenced by the investigation of the kinetics of oxidative addition of PhI with $\text{Pd}^0(\text{PPh}_3)_4$ in the presence of CO (retarding effect of CO) [16].

In the presence of PPh_3 (2 equiv) and CO , the voltammogram of $\text{PdBr}_2(\text{PPh}_3)_2$ exhibited the only reduction peak R_1 (Fig. 1b), because the equilibrium in Eq. (7) was shifted towards its left hand-side due to the excess PPh_3 . On the reverse scan, a single oxidation peak was detected at O_4 ($E_{O_4}^p = +0.245 \text{ V}$), whose peak current was much higher than that of O_2 (compare Fig. 1a and b).

To characterize the Pd^0 complex that was oxidized at O_4 , a set of experiments was performed with an



Scheme 1.

authentic sample of $\text{Pd}^0(\text{PPh}_3)_4$, which contains 4 equiv PPh_3 per Pd^0 as when $\text{PdBr}_2(\text{PPh}_3)_2$ was reduced in the presence of 2 equiv PPh_3 . In THF, $\text{Pd}^0(\text{PPh}_3)_4$ dissociates to $\text{Pd}^0(\text{PPh}_3)_3$, $\text{SPd}^0(\text{PPh}_3)_3$ and $\text{SPd}^0(\text{PPh}_3)_2$ (Scheme 1, S = solvent) [17].

This is why the voltammogram of $\text{Pd}^0(\text{PPh}_3)_4$ (2 mM) in THF (containing $n\text{Bu}_4\text{NBF}_4$, 0.3 M) exhibited two close oxidation peaks O'_1 ($E_{O'_1}^p = +0.245$ V) and O'_2 ($E_{O'_2}^p = +0.375$ V) (Fig. 2a) assigned to $\text{Pd}^0(\text{PPh}_3)_3$ and $\text{SPd}^0(\text{PPh}_3)_3$ involved in the equilibrium of Scheme 1 [17]. When Br^- ions (2 equiv) were added to $\text{Pd}^0(\text{PPh}_3)_4$, the two oxidation peaks O'_1 and O'_2 disappeared to give rise to a single oxidation peak O_1 (Fig. 2b), already obtained when $\text{PdBr}_2(\text{PPh}_3)_2$ was reduced in the presence of 2 equiv PPh_3 and which characterized the oxidation of the anionic Pd^0 complexes $[\text{Pd}^0(\text{PPh}_3)_n\text{Br}]^-$ ($n = 2$ and 3) involved in the equilibrium in Eq. (6). When CO was bubbled into the solution of $\text{Pd}^0(\text{PPh}_3)_4$ (2 mM) in THF containing 2 equiv Br^- , a new broad oxidation peak developed at O_4 ($E_{O_4}^p = +0.245$ V) (Fig. 2c), attesting the complexation of the $[\text{Pd}^0(\text{PPh}_3)_n\text{Br}]^-$ complexes by CO to form less easily oxidized neutral complexes $\text{Pd}^0(\text{PPh}_3)_n(\text{CO})$ ($n = 2$ and 3) (Eq. (10)) – for the existence and characterization of $\text{Pd}^0(\text{PPh}_3)_n(\text{CO})$ complexes, see [18]. The oxidation peak O_4 is similar to that observed when $\text{PdBr}_2(\text{PPh}_3)_2$ was reduced in the presence of CO and 2 equiv PPh_3 (Fig. 1b).



In another set of experiments, CO was first added to $\text{Pd}^0(\text{PPh}_3)_4$. A broad oxidation peak O'_4 was observed at $E_{O'_4}^p = +0.485$ V which characterized the oxidation of the $\text{Pd}^0(\text{PPh}_3)_n(\text{CO})$ ($n = 2$ and 3) complexes involved in the equilibrium of Eq.(10). After addition of 2 equiv Br^- , the broad oxidation peak O'_4 disappeared and the only peak O_4 ($E_{O_4}^p = +0.241$ V) was detected. Since we have seen above that Br^- was released from anionic $[\text{Pd}^0(\text{PPh}_3)_2\text{Br}]^-$ in the presence of CO, the peak O_4 characterized the oxidation of

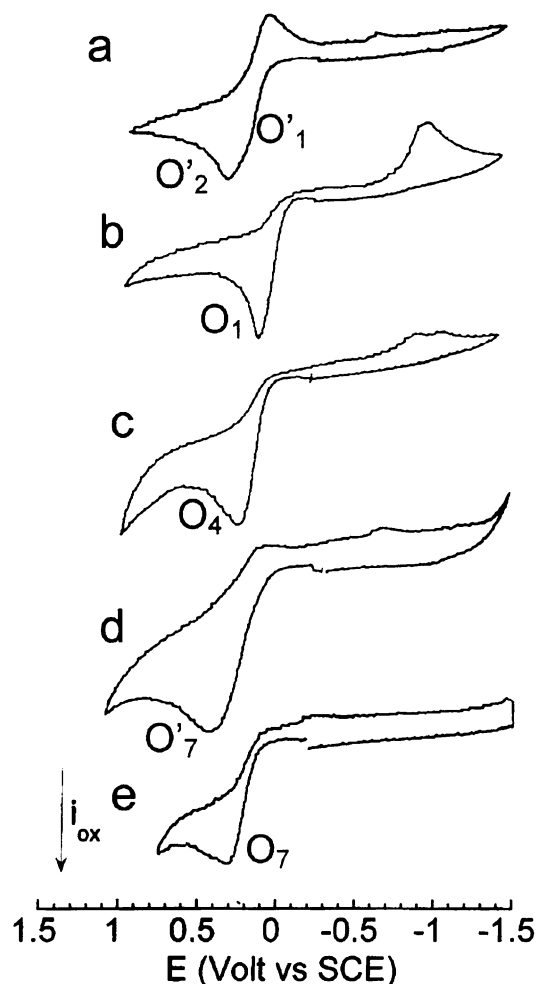
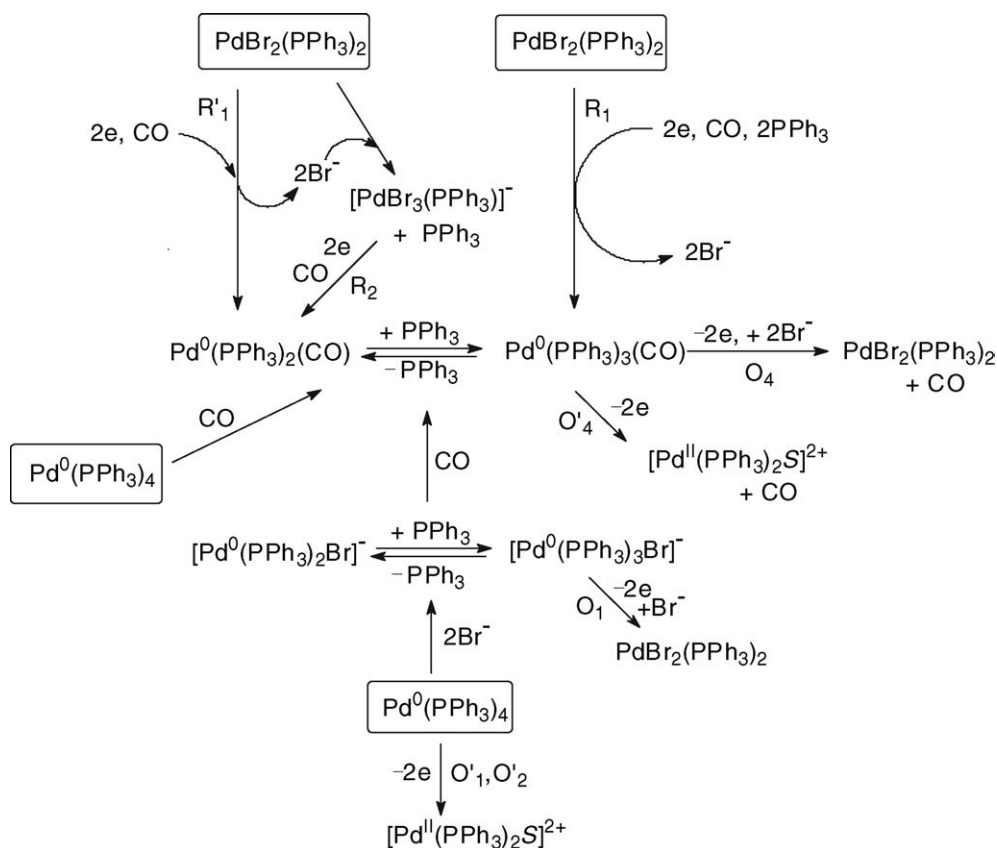


Fig. 2. Cyclic voltammetry performed in THF (containing $n\text{Bu}_4\text{NBF}_4$, 0.3 mol dm^{-3}) at a steady gold disk electrode (i.d. 0.5 mm) with a scan rate of 0.2 V s^{-1} at 25 °C. Oxidation first: (a) $\text{Pd}^0(\text{PPh}_3)_4$ (2 mmol dm^{-3}), (b) $\text{Pd}^0(\text{PPh}_3)_4$ (2 mmol dm^{-3}) and $n\text{Bu}_4\text{NBr}$ (4 mmol dm^{-3}), (c) $\text{Pd}^0(\text{PPh}_3)_4$ (2 mmol dm^{-3}), $n\text{Bu}_4\text{NBr}$ (4 mmol dm^{-3}) and CO (1 atm), (d) $\text{Pd}^0(\text{PPh}_3)_4$ (2 mmol dm^{-3}), EtONa (16 mmol dm^{-3}) and CO (1 atm), (e) $\text{Pd}^0(\text{PPh}_3)_4$ (2 mmol dm^{-3}), $n\text{Bu}_4\text{NBr}$ (4 mmol dm^{-3}) EtONa (16 mmol dm^{-3}) and CO (1 atm).

$\text{Pd}^0(\text{PPh}_3)_n(\text{CO})$ ($n = 2$ and 3) in the presence of Br^- . The observed potential shift from O'_4 to O_4 was therefore mostly due to the chemical reaction of Br^- with the transient Pd^{I} electrogenerated in the first electron oxidation of $\text{Pd}^0(\text{PPh}_3)_n(\text{CO})$ ($n = 2, 3$) (EC mechanism). The potential of an irreversible peak depends on the rate of the chemical step that follows the first electron transfer. In the present case, the first electron transfer gives a cationic Pd^{I} complex involved in a chemical



reaction with Br^- ions. This transient ‘ $\text{Pd}^{\text{I}}\text{Br}^-$ ’ complex is more easily oxidized than the initial Pd^0 . This results in an overall bi-electronic oxidation process occurring at the oxidation potential of Pd^0 , which gives eventually a Pd^{II} complex. For the mechanism of the electrochemical oxidation of Pd^0 complexes, see [19]. The above results are summarized in Scheme 2.

Whatever the Pd^0 precursor, $\text{Pd}^0(\text{PPh}_3)_4$ and 2 equiv Br^- or the Pd^0 complex generated by the electrochemical reduction of $\text{PdBr}_2(\text{PPh}_3)_2$ in the presence of 2 equiv PPh_3 , the introduction of CO generates $\text{Pd}^0(\text{PPh}_3)_n(\text{CO})$ ($n = 2$ and 3) complexes which are oxidized at O_4 ($E_{\text{O}_4}^{\text{p}} = +0.245$ V, Figs. 1b and 2c).

At room temperature and under atmospheric pressure, CO does not coordinate $\text{PdBr}_2(\text{PPh}_3)_2$ and does not reduce $\text{PdBr}_2(\text{PPh}_3)_2$. The only evolution of $\text{PdBr}_2(\text{PPh}_3)_2$ would then be its reduction by the anions ethoxide generated from EtOH in the cathodic process (Eq. (3)).

2.2. Reduction of $\text{PdBr}_2(\text{PPh}_3)_2$ by ethoxide ions in the absence and presence of PPh_3 (2 equiv)

The fate of $\text{PdBr}_2(\text{PPh}_3)_2$ in the presence of excess EtONa (used to mimic the effect of EtO^- electrogenerated at the cathode in the catalytic reaction) was monitored by cyclic voltammetry in THF. The oxidation potential of EtO^- was observed at +1.175 V in THF.

When 8 equiv EtO^- were added to a solution of $\text{PdBr}_2(\text{PPh}_3)_2$ (2 mM) in THF, its reduction peak R_1 disappeared and a succession of oxidation peaks were observed (Fig. 3), whereas the solution turned black. This suggests that $\text{PdBr}_2(\text{PPh}_3)_2$ was reduced by the ethoxide to a multitude of Pd^0 complexes or clusters due to a lack of stabilizing ligands.

To observe stable Pd^0 complex(es) detectable in cyclic voltammetry, the chemical reduction of $\text{PdBr}_2(\text{PPh}_3)_2$ by the ethoxide was performed in the presence of two equiv PPh_3 . The reduction of $\text{PdBr}_2(\text{PPh}_3)_2$ by 2 equiv EtO^- was a slow reaction as

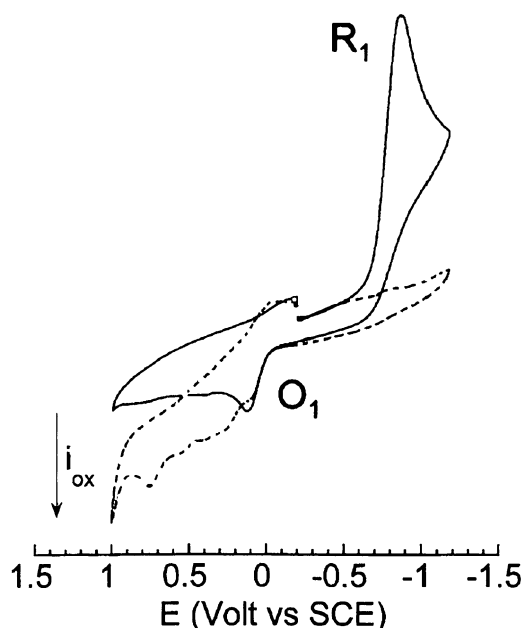


Fig. 3. Cyclic voltammetry performed in THF (containing $n\text{Bu}_4\text{NBF}_4$, 0.3 mol dm^{-3}) at a steady gold disk electrode (i.d. 0.5 mm) with a scan rate of 0.2 V s^{-1} at 25°C . Reduction first: (—) $\text{PdBr}_2(\text{PPh}_3)_2$ (2 mmol dm^{-3}); (---) $\text{PdBr}_2(\text{PPh}_3)_2$ (2 mmol dm^{-3}) and EtONa (16 mmol dm^{-3}).

attested by the slow decay of the reduction peak of $\text{PdBr}_2(\text{PPh}_3)_2$. A large excess EtO^- (8 equiv) was required to reduce $\text{PdBr}_2(\text{PPh}_3)_2$ quantitatively within a reasonable time (1 h 30). Fig. 4a exhibits the reduction peak of $\text{PdBr}_2(\text{PPh}_3)_2$ in the presence of 2 equiv PPh_3 . When 8 equiv EtO^- were added, the reduction peak current of $\text{PdBr}_2(\text{PPh}_3)_2$ decreased (Fig. 4b, reaction time: 35 min) attesting a reaction of $\text{PdBr}_2(\text{PPh}_3)_2$ with EtO^- . An oxidation peak was observed on the reverse scan at a potential close to that of O_1 , but with a higher current intensity than initially (compare Fig. 4a and b), attesting that a Pd^0 complex was generated by the reaction of EtO^- with $\text{PdBr}_2(\text{PPh}_3)_2$. This Pd^0 complex was indeed detected by its oxidation peak O_5 when the voltammetry was performed directly towards positive potentials, without scanning over peak R_1 (Fig. 4c). The complete reduction of $\text{PdBr}_2(\text{PPh}_3)_2$ by EtO^- was achieved within 1 h and a half and the resulting Pd^0 was oxidized at O_5 ($E^p_{\text{O}_5} = +0.090 \text{ V}$).

Due to the close vicinity of the oxidation potentials of O_1 and O_5 , it is difficult to conclude from the cyclic voltammetry whether the Pd^0 generated by the chemical reduction of $\text{PdBr}_2(\text{PPh}_3)_2$ was still ligated by Br^-

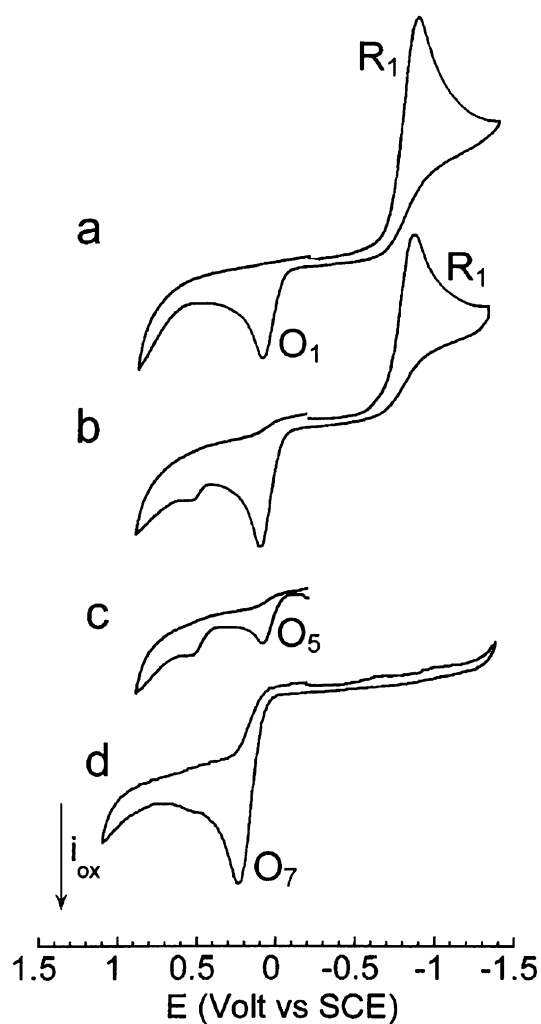
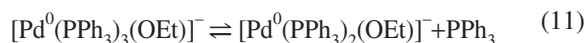


Fig. 4. Cyclic voltammetry performed in THF (containing $n\text{Bu}_4\text{NBF}_4$, 0.3 mol dm^{-3}) at a steady gold disk electrode (i.d. 0.5 mm) with a scan rate of 0.2 V s^{-1} at 25°C . Reduction first: (a) $\text{PdBr}_2(\text{PPh}_3)_2$ (2 mmol dm^{-3}) and PPh_3 (4 mmol dm^{-3}); (b) $\text{PdBr}_2(\text{PPh}_3)_2$ (2 mmol dm^{-3}), PPh_3 (4 mmol dm^{-3}) and EtONa (16 mmol dm^{-3}), 35 min after addition of EtONa ; (c) oxidation first: $\text{PdBr}_2(\text{PPh}_3)_2$ (2 mmol dm^{-3}), PPh_3 (4 mmol dm^{-3}) and EtONa (16 mmol dm^{-3}), 40 min after addition of EtONa ; (d) reduction first: $\text{PdBr}_2(\text{PPh}_3)_2$ (2 mmol dm^{-3}), PPh_3 (4 mmol dm^{-3}), EtONa (16 mmol dm^{-3}) and CO (1 atm) after 1 h 30.

or by EtO^- . Alcazar-Roman and Hartwig have reported kinetic evidence of the formation of anionic Pd^0 complexes ligated by alkoxides [20]. To better characterize the Pd^0 complex generated by the chemical reduction, EtO^- (8 equiv) was added to a solution of $\text{Pd}^0(\text{PPh}_3)_4$ (2 mM) in THF. The two oxidation peaks O'_1 ($+0.245 \text{ V}$) and O'_2 ($+0.375 \text{ V}$) characteristic of $\text{Pd}^0(\text{PPh}_3)_3$ and

$\text{SPd}^0(\text{PPh}_3)_3$ [17] were slightly shifted to more positive potentials O'_5 (+0.265 V) and O'_6 (+0.385 V) respectively. One would have expected to observe less positive oxidation potentials for the putative anionic $[\text{Pd}^0(\text{PPh}_3)_n(\text{OEt})]^-$ species. However, the electrochemical oxidation of anionic $[\text{Pd}^0(\text{PPh}_3)_n(\text{OEt})]^-$ species in the presence of EtO^- must be a complex process as attested by the irreversibility of the oxidation peaks. The formation of anionic $[\text{Pd}^0(\text{PPh}_3)_n(\text{OEt})]^-$ ($n = 2$ and 3) complexes was better supported by ^{31}P NMR experiments. Indeed, the broad ^{31}P NMR signal at +3.23 ppm characteristic of $\text{Pd}^0(\text{PPh}_3)_n$ ($n = 2$ and 3) in equilibrium with PPh_3 , generated from $\text{Pd}^0(\text{PPh}_3)_4$ (7.9 mM) in THF (Scheme 1), was shifted to -3.0 ppm by addition of EtO^- (8 equiv). The signal of the free phosphine was not observed. This shows that EtO^- interfered in the equilibrium of Scheme 1, to form anionic species (Eq. (11)), as already established for halides or acetates [21].

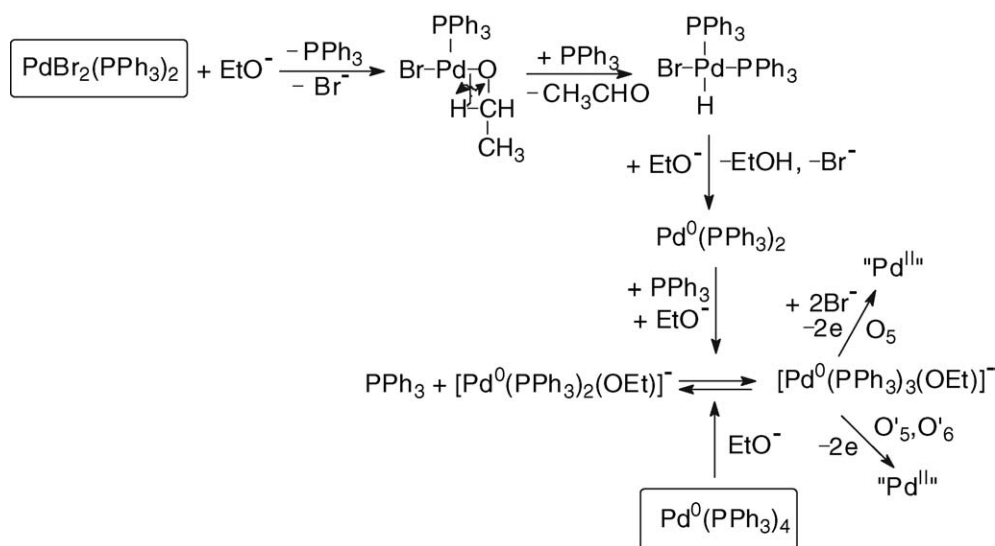


The chemical reduction of $\text{PdBr}_2(\text{PPh}_3)_2$ requires two equivalents of EtO^- and the mechanism involves a classical β -hydride elimination [22], leading to a hydrido-Pd^{II} complex, whose HBr elimination by the basic ethoxide generates a Pd^0 complex stabilized by excess EtO^- and PPh_3 (Scheme 3).

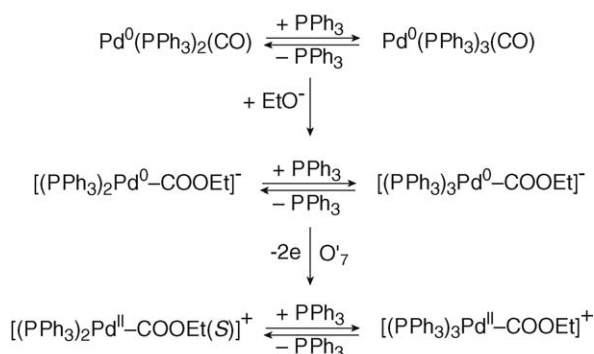
2.3. Reaction of ethoxide ions with $\text{Pd}^0(\text{PPh}_3)_n(\text{CO})$ complexes

According to Scheme 2, $\text{Pd}^0(\text{PPh}_3)_n(\text{CO})$ ($n = 2$ and 3) complexes were generated in the absence of EtO^- , whereas $[\text{Pd}^0(\text{PPh}_3)_n(\text{OEt})]^-$ complexes were formed in the absence of CO (Scheme 3). Taking into account the fact that (i) CO is a better ligand than EtO^- for the electron rich $\text{Pd}^0(\text{PPh}_3)_2$ complex and that (ii) CO is present in large amount in the very first step of the electrolysis whereas EtO^- is generated only when the electrolysis proceeds (Eq. (3)), we favour the formation of $\text{Pd}^0(\text{PPh}_3)_2(\text{CO})$ as the main Pd^0 complex in the very first step of the electrolysis (performed in the absence of PPh_3) rather than that of $[\text{Pd}^0(\text{PPh}_3)_2(\text{OEt})]^-$. It was thus of interest to investigate the reaction of EtO^- with $\text{Pd}^0(\text{PPh}_3)_n(\text{CO})$ complexes, which was monitored in parallel by ^{31}P NMR spectroscopy and cyclic voltammetry.

$\text{Pd}^0(\text{PPh}_3)_n(\text{CO})$ ($n = 2$ and 3) complexes were first generated by bubbling CO into a solution of $\text{Pd}^0(\text{PPh}_3)_4$ (8 mM) in THF and characterized by a broad ^{31}P NMR signal at +7.43 ppm (Eq. (10)) and the broad oxidation peak O'_4 ($E^p_{O'_4} = +0.485$ V) already mentioned above. Addition of EtO^- (8 equiv) generated a new broad signal at +4.15 ppm and a new oxidation peak at less positive potential O'_7 ($E^p_{O'_7} = +0.415$ V) (Fig. 2d), i.e., new species. The reaction of strong nucleophiles such as alkoxydes RO^-



Scheme 3.



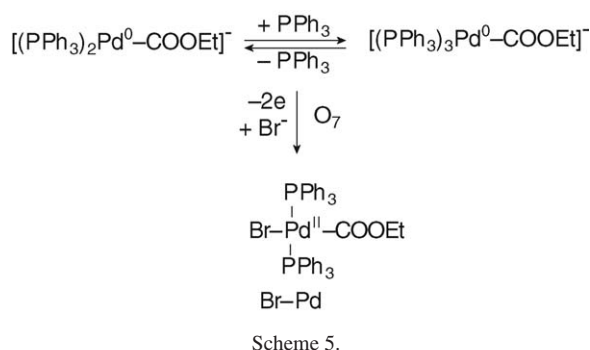
Scheme 4.

with $\text{M}^0(\text{CO})_n$ complexes is a known process that involves the nucleophilic attack of one CO ligand to form anionic alkoxycarbonyl $[(\text{CO})_{n-1}\text{M}^0(\text{COOR})]^-$ complexes [23,24]. In the present case, anionic Pd^0 complexes $[(\text{PPh}_3)_n\text{Pd}^0\text{-COOEt}]^-$ ($n = 2$ and 3) would be generated (Scheme 4). The reaction was monitored by IR spectroscopy. The CO vibration in $\text{Pd}^0(\text{PPh}_3)_3(\text{CO})$ appeared at 2019 cm^{-1} in THF, close to that reported for the solid (1955 cm^{-1}) [18]. When EtO^- was added to $\text{Pd}^0(\text{PPh}_3)_3(\text{CO})$, a new absorption developed at 1650 cm^{-1} , characteristic of COOEt ligated to a palladium centre [11].

The bielectronic oxidation of $[(\text{PPh}_3)_n\text{Pd}^0\text{-COOEt}]^-$ ($n = 2$ and 3) at O'_7 is expected to generate cationic Pd^{II} complexes $[(\text{PPh}_3)_n\text{Pd}^{\text{II}}\text{-COOEt}]^+$ ($n = 2$ and 3) (Scheme 4).

When 2 equiv of Br^- were added to the solution containing of $[(\text{PPh}_3)_n\text{Pd}^0\text{-COOEt}]^-$ ($n = 2$ and 3), the oxidation peak O'_7 ($E_{\text{O}'_7}^{\text{p}} = +0.415 \text{ V}$) observed in Fig. 2d was replaced by a new one O_7 located at less positive potential ($E_{\text{O}_7}^{\text{p}} = +0.215 \text{ V}$) (Fig. 2e). The easier oxidation of $[(\text{PPh}_3)_n\text{Pd}^0\text{-COOEt}]^-$ ($n = 2$ and 3) in the presence of Br^- is most certainly featuring the chemical reaction of the bromide ion with the transient Pd^{I} formed in the first electron transfer (EC mechanism). After an overall bielectronic process, a neutral Pd^{II} complex $\text{BrPd}^{\text{II}}\text{-COOEt}(\text{PPh}_3)_2$ should be generated ultimately (Scheme 5). Related complexes $\text{ClPd-COOR}(\text{PPh}_3)_2$ are reported in literature. They have been synthesized by either the oxidative addition of Cl-COOR to $\text{Pd}^0(\text{PPh}_3)_4$ [11,25,26].

The same oxidation peak O_7 was also observed when $\text{PdBr}_2(\text{PPh}_3)_2$ was reduced by EtO^- in the presence of PPh_3 (2 equiv) and CO (Fig. 4d).

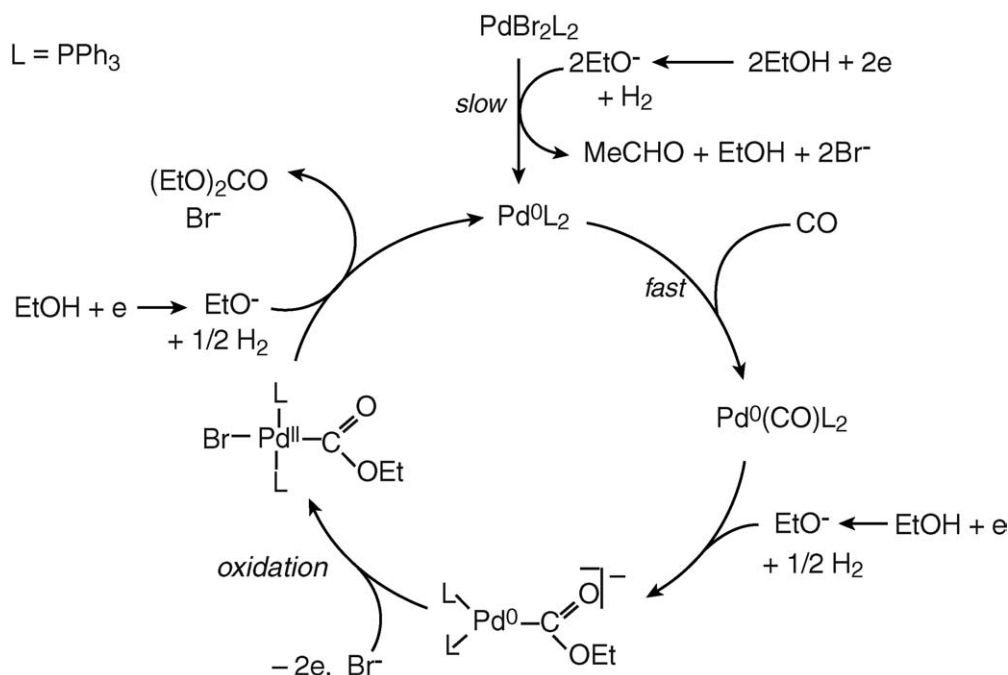


Scheme 5.

2.4. Mechanism of the palladium-catalysed electrosynthesis of diethyl carbonate from carbon monoxide and ethanol

The above mechanistic investigations were developed in THF and in the presence of excess PPh_3 , so that to have a chance to observe and characterize relatively stable Pd^0 complexes and to be able to monitor their evolution in the presence of the reagents involved in the catalytic process. The electrosynthesis of diethyl carbonate proceeds in ethanol and in the absence of extra PPh_3 [3]. The catalyst $\text{PdBr}_2(\text{PPh}_3)_2$ was not tested in the electrosynthesis of diethyl carbonate but a related complex $\text{PdCl}_2(\text{PPh}_3)_2$. The latter was also successfully used in the electrocarbonylation of benzylamine to dibenzylurea [27]. A catalytic cycle for the electrosynthesis performed in ethanol is proposed in Scheme 6.

The chemical reduction of the catalytic precursor $\text{PdBr}_2(\text{PPh}_3)_2$ by the EtO^- generated in the cathodic process gives a Pd^0 that is probably not ligated by neither Br^- nor EtO^- , but by CO. Indeed, the slow chemical reduction proceeds in the presence of CO and, as mentioned above, the concentration of CO in the electrolysis is constant (bubbling CO) and is always higher than that of EtO^- anions. The latter are generated at the cathode and their concentration is controlled by the current density as well as by their chemical consumption. Indeed, once EtO^- ions have reduced the $\text{PdBr}_2(\text{PPh}_3)_2$ to Pd^0 , they are also consumed in a chemical reaction with $\text{Pd}^0(\text{PPh}_3)_2(\text{CO})$. This reaction gives the anionic complex $[(\text{PPh}_3)_2\text{Pd}^0\text{-COOEt}]^-$. The key step of the anodic process is thus the overall bielectronic oxidation of $[(\text{PPh}_3)_2\text{Pd}^0\text{-COOEt}]^-$. This oxidation is conducted in the presence of Br^- delivered by the precursor $\text{PdBr}_2(\text{PPh}_3)_2$. Consequently, it should generate the neutral complex Br-Pd

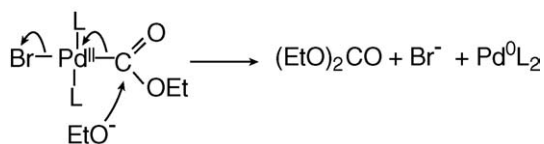
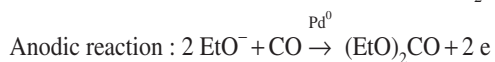


Scheme 6.

$\text{Pd}^{\text{II}}\text{-COOEt}(\text{PPh}_3)_2$ rather than the cationic complex $[(\text{PPh}_3)_2\text{Pd}^{\text{II}}\text{-COOEt}(\text{S})]^+$.

The last step of the catalytic cycle is a nucleophilic attack of the COOEt ligand of $\text{BrPd}^{\text{II}}\text{-COOEt}(\text{PPh}_3)_2$ by EtO^- , as detailed in Scheme 7. This reaction is supported by reported nucleophilic attack of methanol on related complexes, $(\text{AcO})\text{Pd}^{\text{II}}\text{-COOMe}(\text{PPh}_3)_2$, which yields dimethyl carbonate only in the presence of a base [11].

The mechanism of the palladium-catalysed electrocatalytic synthesis of diethyl carbonate from carbon monoxide and ethanol described in Scheme 6 indicates that the anodic and cathodic reactions are interfering. As a result of the mechanistic investigation, the two processes may be expressed as:



Scheme 7.

In the presence of bromide ions, which occurs in the electrolysis because of the catalytic precursor $\text{PdBr}_2(\text{PPh}_3)_2$, the oxidation potential of $\text{Pd}^0(\text{PPh}_3)_2(\text{CO})$ ($E^{\text{p}}_{\text{O}4} = +0.245 \text{ V}$) and that of $[(\text{PPh}_3)_2\text{Pd}^0\text{-COOEt}]^-$ ($E^{\text{p}}_{\text{O}7} = +0.215 \text{ V}$) are very close. If the nucleophilic attack of $\text{Pd}^0(\text{PPh}_3)_2(\text{CO})$ by EtO^- is not fast enough (it is limited by the rate of production of EtO^- at the cathode) the oxidation of $\text{Pd}^0(\text{PPh}_3)_2(\text{CO})$ will also occur leading back to $\text{PdBr}_2(\text{PPh}_3)_2$ and consequently would contribute to lower the faradic efficiency.

3. Conclusion

A mechanism is proposed for the electrocatalytic synthesis of diethyl carbonate from carbon monoxide and ethanol catalysed by $\text{PdBr}_2(\text{PPh}_3)_2$, proceeding at room temperature and under atmospheric CO pressure (Scheme 6). The cathodic and anodic processes have been defined. $\text{PdBr}_2(\text{PPh}_3)_2$ does not react with CO but is reduced by EtO^- . The catalytic cycle involves a succession of neutral or anionic Pd^0 and Pd^{II} complexes generated in chemical steps or in electrochemical oxidation steps.

4. Experimental

The ^{31}P NMR spectra were recorded on a Bruker spectrometer (162 MHz) using H_3PO_4 as an external reference. IR spectra were recorded on a Nicolet Impact 400D spectrometer. Cyclic voltammetry was performed with a homemade potentiostat and a waveform generator GSTP4 (Radiometer Analytical). The voltammograms were recorded with an oscilloscope Nicolet 301.

All experiments were performed using standard Schlenk techniques under argon atmosphere. THF was distilled on potassium/benzophenone. PPh_3 , anhydrous $n\text{Bu}_4\text{NBr}$, and ethanol, sodium ethoxide were commercial (Aldrich) and used without purification. $\text{PdBr}_2(\text{PPh}_3)_2$ [13] and $\text{Pd}^0(\text{PPh}_3)_4$ [28] was synthesized according to published procedures.

4.1. Electrochemical set-up for cyclic voltammetry

Electrochemical experiments were carried out in a three-electrode cell connected to a Schlenk line. The cell was thermostated at 25 °C. The steady working electrode consisted of a gold disk (i.d. 0.5 mm). The counter electrode was a platinum wire of ca 1-cm² apparent surface area. The reference was a saturated calomel electrode separated from the solution by a bridge filled with a solution of $n\text{Bu}_4\text{NBF}_4$ (0.3 mol dm⁻³) in 3 ml of THF. 12 ml of THF containing the same concentration of supporting electrolyte was poured into the cell followed by 17 mg (0.024 mmol) of $\text{PdBr}_2(\text{PPh}_3)_2$ and 12.5 mg (0.048 mmol) of PPh_3 , when required.

In other experiments, 13 mg (0.19 mmol) of EtONa were added to the solution of $\text{PdBr}_2(\text{PPh}_3)_2$ in the absence or presence of bubbling CO.

The cyclic voltammetry was also performed on solutions of 28 mg (0.024 mmol) $\text{Pd}^0(\text{PPh}_3)_4$ alone and then in the presence of 13 mg (0.19 mmol) of EtONa in the absence or presence of bubbling CO. When required, 15.5 mg (0.048 mmol) of $n\text{Bu}_4\text{NBr}$ were added.

Acknowledgements

This work has been supported in part by the ‘Centre national de la recherche scientifique’ (CNRS, UMR

8640 ‘PASTEUR’), the ‘Ministère de la Recherche (‘École normale supérieure’) and the University Paris-6. We thank Johnson Matthey for a generous loan of sodium tetrachloropalladate.

References

- [1] A. Galia, G. Filardo, S. Gambino, R. Mascolino, F. Rivetti, G. Silvestri, *Electrochim. Acta* 41 (1996) 2893.
- [2] G. Filardo, A. Galia, F. Rivetti, O. Scialdone, G. Silvestri, *Electrochim. Acta* 42 (1997) 1961.
- [3] A. Galia, G. Filardo, O. Scialdone, M. Musacco, G. Silvestri, in: S. Torii (Ed.), *Novel Trends in Electroorganic Synthesis*, 42, Springer-Verlag, Tokyo, 1998, p. 3.
- [4] D.M. Fenton, US Patent, 3 227 740, 1963.
- [5] E. Perrotti, G. Cipriani, US Patent, 3 848 468, 1971.
- [6] D.M. Fenton, P.J. Steinwand, *J. Org. Chem.* 39 (1974) 701.
- [7] K. Otsuka, T. Yagi, I. Yamanaka, *Chem. Lett.* (1994) 495.
- [8] K. Otsuka, T. Yagi, I. Yamanaka, *Electrochim. Acta* 39 (1994) 2109.
- [9] F. Rivetti, U. Romano, *J. Organomet. Chem.* 154 (1978) 323.
- [10] F. Rivetti, U. Romano, *J. Organomet. Chem.* 174 (1979) 221.
- [11] R. Bertani, G. Cavinato, L. Toniolo, G. Vasapollo, *J. Mol. Catal.* 84 (1993) 165.
- [12] G. Cavinato, L. Toniolo, *J. Organomet. Chem.* 444 (1993) C65.
- [13] C. Amatore, M. Azzabi, A. Jutand, *J. Am. Chem. Soc.* 113 (1991) 8375.
- [14] C. Amatore, A. Jutand, L. Mottier, *Eur. J. Inorg. Chem.* (1999) 1081.
- [15] M. Graziani, P. Uguagliati, G. Carturan, *J. Organomet. Chem.* 27 (1971) 275.
- [16] I. Carelli, I. Chiarotto, S. Cacchi, P. Pace, C. Amatore, A. Jutand, G. Meyer, *Eur. J. Org. Chem.* (1999) 1471.
- [17] C. Amatore, A. Jutand, F. Khalil, M.A. M'Barki, L. Mottier, *Organometallics* 12 (1993) 3168.
- [18] K. Kudo, M. Hidai, Y. Uchida, *J. Organomet. Chem.* 33 (1971) 393.
- [19] C. Amatore, A. Jutand, M.-J. Medeiros, L. Mottier, *J. Electroanal. Chem.* 422 (1997) 125.
- [20] L.M. Alcazar-Roman, J. Hartwig, *J. Am. Chem. Soc.* 123 (2001) 12905.
- [21] C. Amatore, A. Jutand, *Acc. Chem. Res.* 33 (2000) 314.
- [22] P.J. Davidson, M.F. Lappert, R. Pearce, *Chem. Rev.* 76 (1976) 219.
- [23] J.P. Collman, L.S. Hegeudus, J.R. Norton, R.G. Finke, *Principles and Applications of Organotransition Metal Chemistry*, Oxford University Press, 1987, p. 403.
- [24] R.J. Angelici, *Acc. Chem. Res.* 5 (1972) 335.
- [25] S. Otsuka, A. Nakamura, T. Yoshida, M. Naruto, K. Ataka, *J. Am. Chem. Soc.* 95 (1973) 3180.
- [26] E.D. Dobrzynski, R.J. Angelici, *Inorg. Chem.* 14 (1975) 59.
- [27] D. Fenech, A. Galia, G. Silvestri, unpublished results.
- [28] D.T. Rosevear, F.G.A. Stone, *J. Chem. Soc. A* (1968) 164.